Available online at www.sciencedirect.com
SCIENCE DIRECT®
Journal of Organometallic Chemistry 689 (2004) 3093–3107
Journal of Organometallic Chemistry
www.elsevier.com/locate/jorganchem

Lithium and sodium *N*,*N*′-di(2,6-dialkylphenyl)formamidinate complexes

Marcus L. Cole [a,1], Aaron J. Davies [a,2], Cameron Jones [b], Peter C. Junk [a,*]

[a] *School of Chemistry, Monash University, Victoria 3800, Australia*
[b] *Department of Chemistry, Cardiff University, Park Place, P.O. Box 912, Cardiff CF10 3TB, UK*

Received 13 May 2004; accepted 1 July 2004
Available online 5 August 2004

Abstract

A study has been undertaken of the lithium and sodium metallation of *N*,*N*′-di(aryl)formamidines with alkyl groups at the 2- and 6-aryl position. ^{1}H NMR and X-ray diffraction data indicate an increase in steric bulk from 2,6-dimethylphenyl to 2,6-diethylphenyl to 2,6-diisopropylphenyl incites incremental changes in amidinate binding and nuclearity. In selected instances, this invokes the first lithium and sodium amidinate/guanidinate complexes to exhibit metal–arene contacts.

Keywords: Alkali metals; Amides; N-donor ligands

1. Introduction

The use of sterically encumbered aromatic substituents to isolate kinetically transient low-valent species of the main-group elements [1–6], in particular those of periods four and five, is an area of significant academic interest. In these cases, it is recognised that the steric bulk of such ligands often incites modification of bonding and assembly. By contrast, attempts to apply the same rationale to species of known kinetic and thermodynamic stability in order to observe changes in structure and, more importantly, reactivity have been sparse [7].

Our interest in the application of alkali metal *N*,*N*′-di(aryl)formamidinates ([ArNC(H)NAr]$^-$, Ar = aryl) [8–11] toward the generation of lanthanoid species [12] gave us a special interest in the impact of sterically bulky substituents upon their use as metathesis reagents [13–15]. To date, our study of light alkali metal *N*,*N*′-di(aryl)formamidinates has concentrated mainly upon species of low aryl steric bulk, e.g., *N*,*N*′-di(*para*-tolyl)formamidine (HFTolP) [8–10]. However, as listed in Fig. 1, we have now prepared several new ligands with greater steric encumbrance at the 2- and 6-position of the aromatic ring, e.g. *N*,*N*′-di(2,6-diisopropylphenyl)formamidine (HFIso). Thus far, these have been used in preliminary potassium metallation studies [16,17]. In the case of *N*,*N*′-di(mesityl)formamidine, [3] this led to the partially deprotonated compound [K(η^6:η^1-FMes)(η^6:η^1-HFMes)] [16] (FMes/HFMes = *N*,*N*′-di(mesityl)formamidinate/ine), wherein the metal is bound by imine/amide and η^6-arene interactions from each ligand that create a 'pseudo-metallocene' unit (see Fig. 2). This unusual motif, which is retained in the presence of the bidentate Lewis base donors DME and TMEDA, results from the steric imposition of the

* Corresponding author. Fax: +61 3 9905 4597.
E-mail address: peter.junk@sci.monash.edu.au (P.C. Junk).
[1] Present address: Department of Chemistry, University of Adelaide, Adelaide, South Australia 5005, Australia.
[2] On leave from: Department of Chemistry, Cardiff University, Park Place, P.O. Box 912, Cardiff CF10 3TB, UK.

[3] Mesityl = 2,4,6-trimethylphenyl.

0022-328X/$ - see front matter © 2004 Elsevier B.V. All rights reserved.
doi:10.1016/j.jorganchem.2004.07.004

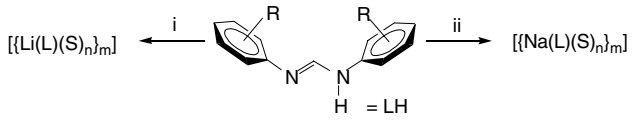

For lithium complexes

R = 2,6-Me_2 (L = FXyl); S = THF(**1**), = DME (**4**)
R = 2,6-Et_2 (L = FPhEt); S = THF(**2**), = DME (**5**)
R = 2,6-^{i}Pr (L = FIso); S = THF(**3**), = DME (**6**)

For sodium complexes

R = 2,6-Me_2 (L = FXyl); S = THF(**7**), = DME (**10**)
R = 2,6-Et_2 (L = FPhEt); S = THF(**8**), = DME (**11**)
R = 2,6-^{i}Pr (L = FIso); S = THF(**9**), = DME (**12**)

Fig. 1. Schematic of *N*,*N*′-di(aryl)formamidines used and numbering of products formed. *Reagents and conditions*: (i) $Bu^{n}Li$, THF or DME, RT, – $Bu^{n}H$ and (ii) Na{$N(SiMe_3)_2$}, THF or DME, RT, – $HN(SiMe_3)_2$.

mesityl groups and the provision of alkyl electron density to the arene donor, the latter strengthening the π-donor to metal interaction. Combined, these interactions suppress deprotonation of the included HFMes moiety and frustrate the conventional μ_2:η^2:η^2-binding exhibited by all other *N*,*N*′-symmetrical amidinate complexes of potassium [18–20]. We have recently discovered that an increase of the mesityl bulk of FMes to 2,6-diisopropyl (HFIso) [17] disrupts the stable [K(formamidine)(formamidinate)] core to render species that are either completely deprotonated or of the form [K(η^6:η^1-formamidinate)(solvent donor)$_n$](formamidine) [17].

Herein, we describe the extension of this work to lithium and sodium, wherein the ligands HFXyl, HFPhEt and HFIso (see Fig. 1), which represent *N*,*N*′-di(2,6-dimethylphenyl-, 2,6-diethylphenyl- and 2,6-diisopropylphenyl)formamidine, respectively, have been deprotonated by either *n*-butyl lithium or sodium bis(trimethylsilyl)amide in tetrahydrofuran (THF) or 1,2-dimethoxyethane (DME). This renders species of empirical formula: [Li(FXyl)$(THF)_{3/2}$] (**1**), [Li(FPhEt)$(THF)_2$], (**2**), [Li(FIso)$(THF)_2$] (**3**), [Li(FXyl)(DME)] (**4**), [Li(FPhEt)(DME)] (**5**), [Li(FIso)(DME)] (**6**), [Na(FXyl)$(THF)_2$] (**7**), [Na(FPhEt)(THF)] (**8**), [Na(FIso)$(THF)_3$] (**9**), [Na(FXyl)$(DME)_2$] (**10**), [Na(FPhEt)(DME)] (**11**) and [Na(FIso)$(DME)_2$] (**12**). The molecular structures of **1**–**3**, **5**, **6** and **8**–**12** have been deduced using single crystal X-ray diffraction methods. These suggest significant structural diversity within the entire lithium and sodium *N*,*N*′-di(aryl)formamidinate catalogue. Complexes **1**–**12** have also been studied spectroscopically (^{1}H and ^{13}C NMR and FTIR).

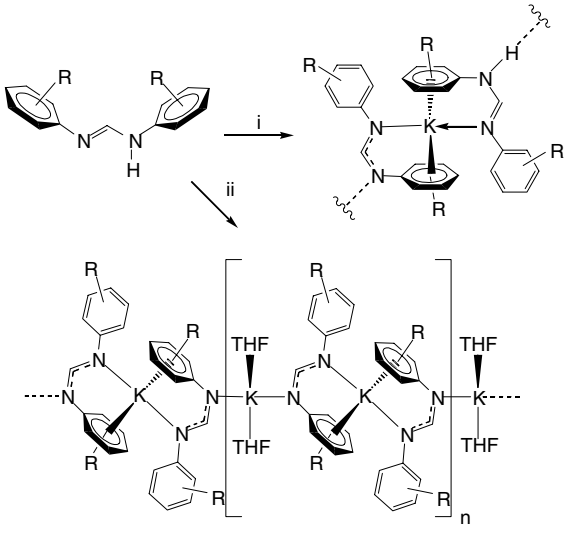

Fig. 2. Previous potassium complexes using *N*,*N*′-di(aryl)formamidinates with 2,6-dialkylaryl substituents. *Reagents and conditions*: (i) R = 2,4,6-Me_3, K{$N(SiMe_3)_2$}, THF/DME/Toluene, RT, –0.5 $HN(SiMe_3)_2$ and (ii) R = 2,6-Pr^{i}_2, K{$N(SiMe_3)_2$}, THF, RT, – $HN(SiMe_3)_2$.

2. Results and discussion

2.1. Lithium complexes

The 1:1 stoichiometric treatment of THF and DME solutions of HFXyl, HFPhEt and HFIso with *n*-butyl lithium results in clean deprotonation of the *N*,*N*′-di(aryl)formamidine amino group (no N–H stretch by FTIR, significant shift in the C=N stretch from 1634, 1635 and 1666 cm^{-1} respectively [21] to 1687 cm^{-1} (**1**), 1660 cm^{-1} (**2**), 1607 cm^{-1} (**3**), 1663 cm^{-1} (**4**), 1661 cm^{-1} (**5**) and 1602 cm^{-1} (**6**)) [22] to render highly air and moisture sensitive species that can be crystallised directly from solution to yield compounds characterising as **1**–**6** (formulation listed above) on the basis of the appropriate resonance signal integration in their ^{1}H NMR spectra (C_6D_6). Unlike the parent *N*,*N*′-di(aryl)formamidines, which exhibit fluxional NMR spectra at ambient temperature due to equilibration between *Z-anti*/*E-syn* and *E-anti* isomers (C_6D_6) [21,23], **1** and **3**–**6** display discrete resonances consistent with a singular isomeric composition. However, the ethyl region of the ^{1}H NMR of compound **2**; [Li(FPhEt)$(THF)_2$], suggests at-least two differing ligand environments, one of which tentatively assigned as a conventional symmetrical *N*,*N*′-binding mode that is typical of metal amidinate species in general [8–11,13–15], and the other an asymmetric *Z-anti*/*E-syn* [23] tautomer on the basis of inequivalent ethyl environments of equal intensity (CH_3 resonances broadened triplets at 1.33, 1.36 and 1.39 ppm in 1:1:2 ratio). This asymmetry, like that observed for related potassium compounds [16,17], might suggest metal-aryl interactions. Alternatively, the presence of more than two heavily congested *E-anti* ligand environments, where the aryl groups may lack chemical equivalency, could be culpable.

Further to spectroscopic characterisation, the isolation of **1**–**6** as crystalline materials permitted the single crystal X-ray structure determinations of **1**–**3**, **5** and **6**. In contrast, high solvent dependency [24] and consistent twinning frustrated the successful acquisition of structural data for **4**. As can be seen in Figs. 3–7 (POV-RAY illustrations, thermal ellipsoids 40%), this permitted full identification of the binding modes present. Table 1 contains a summary of crystallographic data for the lithium compounds characterised by single crystal X-ray crystallography in this work, while Table 2 provides selected bond lengths and angles.

As illustrated in Figs. 3–5, the lithium *N*,*N*′-di(aryl)formamidinate THF species exhibit three contrasting modes of binding. Qualitatively, these progress from a μ_2:η^1:η^1-*N*,*N*′-di(aryl)formamidinate bound dimer for FXyl (Fig. 3, accompanied by two terminal and one bridging THF ligand) [25] to a *pseudo* lithium-lithiate bridged by an unusual *E-syn*/*Z-anti* [23] μ_2:η^1:η^1:η^1-*N*,*C*,*N*′-FPhEt ligand vide infra (Fig. 4,

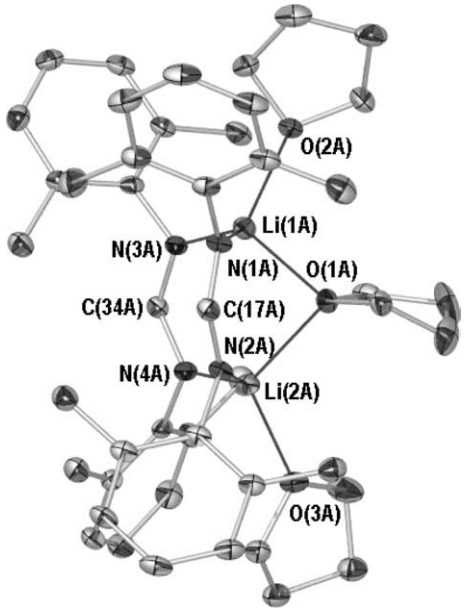

Fig. 3. X-ray crystal structure of one molecular unit of [Li_2(μ_2:η^1:η^1-*N*,*N*′-FXyl)$_2$(μ_2-THF)(THF)$_2$] (**1**). All hydrogen atoms omitted for clarity.

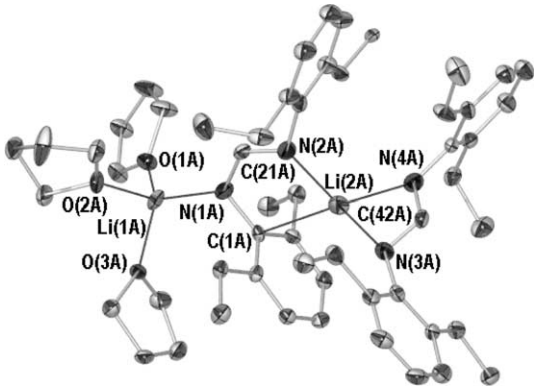

Fig. 4. X-ray crystal structure of one molecular unit of [Li(THF)$_3$(μ_2:η^1:η^1-*N*,*C*,*N*′-FPhEt)Li(η^2-*N*,*N*′-FPhEt)] (**2**). All hydrogen atoms, lattice solvent and lower occupancy disordered atoms omitted for clarity.

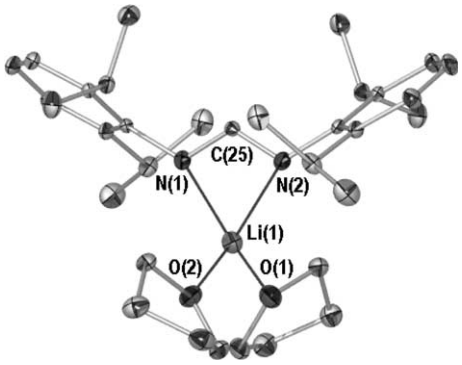

Fig. 5. X-ray crystal structure of [Li(η^2-*N*,*N*′-FIso)(THF)$_2$] (**3**). All hydrogen atoms omitted for clarity.

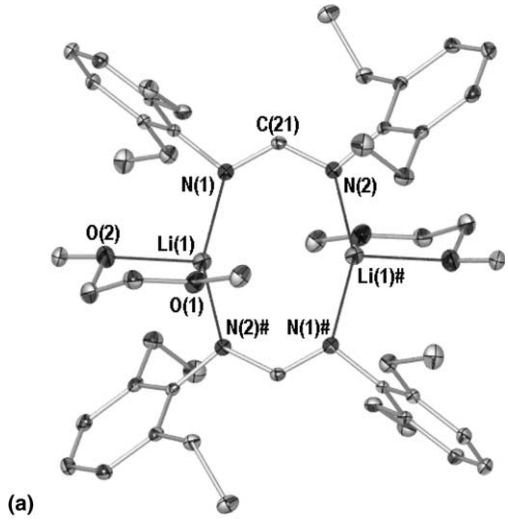

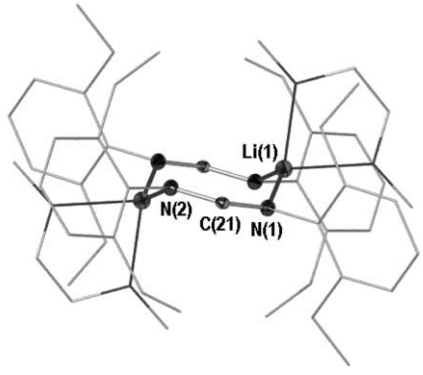

Fig. 6. (a) X-ray crystal structure of [{Li(μ_2:η^1:η^1-*N*,*N*′-FPhEt)(DME)}$_2$] (**5**). All hydrogen atoms omitted for clarity. (b) Orientation of **5** depicting "chair-like" conformation, all non-chair participating atoms and bonds depicted as wire-frames. Symmetry transformation used to generate # atoms: 1/2−*x*, 1/2−*y*, 1−*z*.

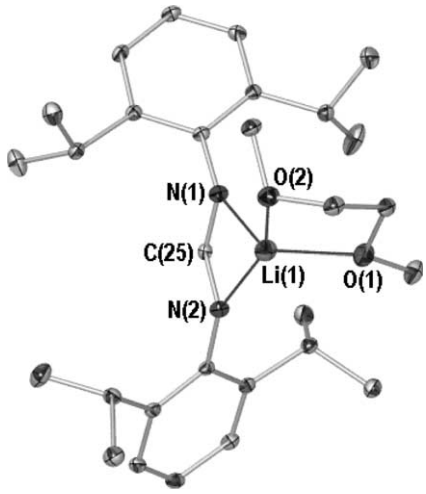

Fig. 7. X-ray crystal structure of [Li(η^2-*N*,*N*′-FIso)(DME)] (**6**). All hydrogen atoms omitted for clarity.

with accompanying η^2-*N*,*N*′-FPhEt), to a simple η^2-*N*,*N*′-bound monomer for FIso (Fig. 5). This bonding describes a gradual trend from bridging to chelating donor. This can be seen from the mean NCN-backbone angles for each species (both **1** and **2** exhibit two molecular units in the asymmetric unit, hence mean values given), which decrease from 125.4° to 126.9°/121.2° (bridging/chelating *N*,*N*′-di(aryl)formamidinates) to 120.0(2)° (**1**–**3** resp.). Making allowances for increases in steric bulk, the mean Li–N bond lengths of 2.050 (**1**), 1.965/2.070 (**2** bridging/chelating) and 2.039 Å (**3**) are also fairly indicative of the mode chosen (mean structurally authenticated lithium to amide nitrogen bond length; 2.078 Å) [26]. The steric buttressing induced by placement of methyl groups at the 2,6-aryl positions can be gauged by the extended lithium to nitrogen interactions of **1** relative to those of the related FTolP species [$Li_2(\mu_2{:}\eta^1{:}\eta^1$-FTolP)$_2(\mu_2$-THF)(THF)$_2$] (2.028 Å) [8], which also exhibits a bridging THF (Li–$O_{bridging}$; 2.053(4)–2.128(4) Å (**1**), 2.093(8) Å (FTolP)) [25]. This bulk also opens the *intra*-ligand aryl:aryl plane torsion angle. For the FTolP species, this is 41.7(2)° [8], while for **1** a mean angle of 71.3° is assumed. For comparison, in **2** and **3** the *N*,*N*′-chelate ligands possess mean aryl:aryl ring torsion angles of 77.2° and 67.7(1)° (resp.), with placement of the aromatic rings toward perpendicular relative to the NCNLi metallocyclic plane (mean dihedral aryl:NCN place angle, **1**; 76.3°, **2**; 61.3°, **3**; 66.7°, FTolP; 40.4°) [8]. This conformation of the aromatic rings frustrates any electronic conjugation across the di(aryl)NCN frame, which otherwise appears to be a prominent feature of less bulky alkali metal *N*,*N*′-di(aryl)formamidinates [8–11,24].

The most novel binding type of compounds **1**–**3** is that of the asymmetric ligand of compound **2** (Fig. 4). This compound possesses both an *E-anti* [23] FPhEt ligand (that of N(3A),N(4A) and N(3B),N(4B)) and a heavily strained $\mu_2{:}\eta^1{:}\eta^1$-*N*,*C*,*N*′-FPhEt *E-syn*/*Z-anti* [23] ligand, for which the tautomerisation cannot be distinguished due to statistically equivalent *intra*-NCN bond lengths of 1.329(5) Å, 1.326(5) Å (C(21A)–N(1A)/N(2A)) and 1.318(5) Å, 1.318(5) Å (C(21B)–N(1B)/N(2B)) (HFPhEt C–N/C=N discrepancy 0.077 Å [21], **1**; C(17A)–N(1A)/N(2A) 1.315(3) Å and 1.326(3) Å resp., **3**; N(1)–C(25) 1.321(3) Å, N(2)–C(25)

Table 1
Summary of crystal data for lithium compounds **1**–**3**, **5** and **6**

	[$Li_2(\mu_2{:}\eta^1{:}\eta^1$-*N*,*N*′-FXyl)$_2$($\mu_2$-THF)(THF)$_2$] (**1**)	[Li(THF)$_3(\mu_2{:}\eta^1{:}\eta^1{:}\eta^1$-*N*,*C*,*N*′-FPhEt)Li($\eta^2$-*N*,*N*′-FPhEt)].THF (**2**)	[Li(η^2-*N*,*N*′-FIso)(THF)$_2$] (**3**)	[{Li($\mu_2{:}\eta^1{:}\eta^1$-*N*,*N*′-FPhEt)(DME)}$_2$] (**5**)	[Li(η^2-*N*,*N*′-FIso)(DME)] (**6**)
Mol. formula	$C_{46}H_{62}N_4O_3Li_2$	$C_{58}H_{86}N_4O_4Li_2$	$C_{33}H_{51}N_2O_2Li_1$	$C_{50}H_{74}N_4O_4Li_2$	$C_{29}H_{45}N_2O_2Li_1$
Mol. weight	1465.75	1834.38	514.70	404.51	460.61
Temperature (K)	123(2)	123(2)	123(2)	123(2)	123(2)
Space group	$P\bar{1}$	$P\bar{1}$	$P\bar{1}$	*C*2/*c*	$P\bar{1}$
a (Å)	10.0831(1)	13.744(3)	10.934(2)	20.661(4)	10.6904(4)
b (Å)	17.8932(2)	20.217(4)	12.100(2)	15.288(3)	10.9257(5)
c (Å)	23.7096(4)	20.924(4)	13.922(3)	15.049(3)	12.7312(6)
α (°)	86.346(1)	108.77(3)	107.09(3)	90	94.928(2)
β (°)	84.674(1)	91.07(3)	97.28(3)	90.68(3)	98.931(2)
γ (°)	89.315(1)	90.46(3)	111.04(3)	90	108.397(2)
Volume (Å^3)	4250.5(1)	5503.1(19)	1586.5(6)	4753.3(16)	1379.4(1)
Z	4	4	2	4	2
D_c (g cm^{-3})	1.145	1.107	1.077	1.130	1.109
μ (mm^{-1})	0.070	0.068	0.065	0.070	0.068
Reflections collected	55,442	57,402	16,417	20,649	24,828
Unique reflections	20,965	26,233	7724	5832	6514
Parameters varied	1007	1303	351	277	317
R_{int}	0.1134	0.2361	0.0709	0.1475	0.0599
R_1	0.0697	0.0860	0.0648	0.0598	0.0489
wR_2	0.1461	0.1157	0.1349	0.1347	0.1024

Table 2
Selected bond lengths (Å) and angles (°) for lithium compounds **1**–**3**, **5** and **6**

Compound ***1***[a]					
Li(1A)–N(1A)	2.044(4)	Li(2A)–N(4A)	2.062(4)	N(1A)–C(17A)	1.315(3)
Li(1A)–N(3A)	2.055(4)	Li(2A)–N(4A)	2.033(4)	N(2A)–C(17A)	1.326(3)
Li(1A)–O(1A)	2.053(4)	Li(2A)–O(1A)	2.114(4)	N(3A)–C(34A)	1.326(3)
Li(1A)–O(2A)	2.031(4)	Li(2A)–O(3A)	2.027(4)	N(4A)–C(34A)	1.313(3)
Li(1A)···Li(2A)	2.885(5)				
N(1A)–Li(1A)–N(3A)	126.6(2)	N(2A)–Li(2A)–N(4A)	129.7(2)	Li(1A)–N(1A)–C(17A)	119.2(2)
N(1A)–Li(1A)–O(1A)	104.3(2)	N(2A)–Li(2A)–O(1A)	97.5(2)	Li(2A)–N(2A)–C(17A)	129.5(2)
N(1A)–Li(1A)–O(2A)	103.1(2)	N(2A)–Li(2A)–O(3A)	112.2(2)	Li(1A)–N(3A)–C(34A)	129.0(2)
N(3A)–Li(1A)–O(1A)	102.1(2)	N(4A)–Li(2A)–O(1A)	104.6(2)	Li(2A)–N(4A)–C(34A)	119.8(2)
N(3A)–Li(1A)–O(2A)	112.6(2)	N(4A)–Li(2A)–O(3A)	101.4(2)	N(1A)–C(17A)–N(2A)	125.8(2)
O(1A)–Li(1A)–O(2A)	106.5(2)	O(1A)–Li(2A)–O(3A)	110.6(2)	N(2A)–C(34A)–N(4A)	125.4(2)
Li(1A)–O(1A)–Li(2A)	87.6(2)				
Compound ***2***[a]					
Li(1A)–N(1A)	1.962(9)	Li(2A)–C(1A)	2.651(9)	N(1A)–C(21A)	1.329(5)
Li(1A)–O(1A)	1.916(10)	Li(2A)–N(2A)	1.956(9)	N(2A)–C(21A)	1.326(5)
Li(1A)–O(2A)	1.968(9)	Li(2A)–N(3A)	2.097(10)	N(3A)–C(42A)	1.331(5)
Li(1A)–O(3A)	1.975(8)	Li(2A)–N(4A)	2.039(9)	N(4A)–C(42A)	1.311(6)
N(1A)–C(1A)	1.422(6)	C(1A)–C(2A)	1.389(6)	C(1A)–C(6A)	1.409(6)
C(2A)–C(3A)	1.404(6)	C(5A)–C(6A)	1.388(6)	C(3A)–C(4A)	1.381(6)
C(4A)–C(5A)	1.380(6)				
N(1A)–Li(1A)–O(1A)	112.3(4)	C(1A)–Li(2A)–N(2A)	70.1(3)	Li(1A)–N(1A)–C(1A)	116.7(4)
N(1A)–Li(1A)–O(2A)	117.4(5)	C(1A)–Li(2A)–N(3A)	128.4(4)	Li(1A)–N(1A)–C(21A)	128.7(4)
N(1A)–Li(1A)–O(3A)	114.9(4)	C(1A)–Li(2A)–N(4A)	146.2(5)	C(1A)–N(1A)–C(21A)	114.4(4)
O(1A)–Li(1A)–O(2A)	106.4(4)	N(2A)–Li(2A)–N(3A)	142.3(5)	Li(2A)–N(2A)–C(21A)	125.7(4)
O(1A)–Li(1A)–O(3A)	104.2(4)	N(2A)–Li(2A)–N(4A)	117.5(4)	N(1A)–C(21A)–N(2A)	126.1(5)
O(2A)–Li(1A)–O(3A)	100.0(4)	N(3A)–Li(2A)–N(4A)	67.6(3)	N(3A)–C(42A)–N(4A)	121.2(5)
Compound ***3***					
Li(1)–N(1)	2.036(4)	Li(1)–O(1)	1.920(5)	N(1)–C(25)	1.321(3)
Li(1)–N(2)	2.041(4)	Li(1)–O(2)	1.929(4)	N(2)–C(25)	1.318(3)
N(1)–Li(1)–N(2)	68.2(1)	N(2)–Li(1)–O(1)	116.5(2)	O(1)–Li(1)–O(2)	109.0(2)
N(1)–Li(1)–O(1)	123.2(2)	N(2)–Li(1)–O(2)	121.9(2)	N(1)–C(25)–N(2)	120.0(2)
N(1)–Li(1)–O(2)	113.6(2)				
Compound ***5***[b]					
Li(1)–N(1)	2.048(3)	Li(1)–O(1)	2.075(3)	N(1)–C(21)	1.316(2)
Li(1)–N(2)#	2.050(3)	Li(1)–O(2)	2.098(3)	N(2)–C(21)	1.324(2)
Li(1)···Li(1)#	3.422(6)				
N(1)–Li(1)–N(2)#	132.8(2)	N(2)#–Li(1)–O(1)	102.8(1)	Li(1)–N(1)–C(21)	128.0(1)
N(1)–Li(1)–O(1)	116.9(2)	N(2)#–Li(1)–O(2)	108.4(1)	Li(1)#–N(2)–C(21)	122.5(1)
N(1)–Li(1)–O(2)	103.4(1)	O(1)–Li(1)–O(2)	79.1(1)	N(1)–C(21)–N(2)	125.9(2)
Compound ***6***					
Li(1)–N(1)	2.028(3)	Li(1)–O(1)	1.973(3)	N(1)–C(25)	1.318(2)
Li(1)–N(2)	2.047(2)	Li(1)–O(2)	2.028(3)	N(2)–C(25)	1.320(2)
N(1)–Li(1)–N(2)	68.4(1)	N(2)–Li(1)–O(1)	120.5(1)	O(1)–Li(1)–O(2)	83.6(1)
N(1)–Li(1)–O(1)	125.0(1)	N(2)–Li(1)–O(2)	153.7(1)	N(1)–C(25)–N(2)	120.4(1)
N(1)–Li(1)–O(2)	108.1(1)				

[a] Two molecular units in the asymmetric unit. Due to similar metrical parameters only molecule "A" listed.
[b] Symmetry transformation used to generate # atoms: $1/2-x$, $1/2-y$, $1-z$.

1.318(3) Å), which infer considerable delocalisation of the negative charge across this unusually contorted diazaallyl fragment. This ambiguity is similarly expressed by the Li–N bond lengths for the two 'potential' lithium amide bonds, which are also statistically identical (Li(1A)–N(1A); 1.962(9) Å, Li(2A)–N(2A); 1.956(9) Å, Li(1B)–N(1B); 1.970(8) Å, Li(2B)–N(2B); 1.972(9) Å). Compound **2** is the first amidinate/guanidinate lithium complex to exhibit metal-arene interactions. The Li–C bond length of the η^1-interaction (Li(2A)–C(1A) 2.651(9) Å, Li(2B)–C(1B) 2.672(9) Å) is well within other structurally authenticated lithium to neutral-arene contacts [27–31], e.g., 2.367(9)–2.707(9) Å in [Sn(2,6-$Trip_2C_6H_3$)$(CH_3)_2$-Sn(2,6-$Trip_2C_6H_3$)(CH_3)(Li)] [29] and 2.38(2)–2.77(2) Å in [Li(μ-S2,6-$Mes_2C_6H_3)_3$] [27] (Trip = 2,4,6-triisopropylphenyl, Mes = 2,4,6-trimethylphenyl). As an aside, the *pseudo* lithium–lithiate composition of **2**, which approaches $[Li(THF)_3]^+$

$[Li(FPhEt)_2]^-$, is reminiscent of the related DME coordinated FTolO species (FTolO = *N*,*N*′-di(*ortho*-tolyl)formamidinate) $[Li(DME)_3][Li(FTolO)_2]$ [11], which exhibits solely η^2-*N*,*N*′-chelate interactions to one lithium centre. Unfortunately, a THF bound analogue of $[Li(DME)_3][Li(FTolO)_2]$ is not available for comparison, however, given the preference of FTolP and FXyl (**1**) to bind lithium as a μ_2:η^1:η^1-dimer (when coordinated by THF) [8], it is likely that the related FTolO species would also participate in this structural type. Certainly, however, the solid-state binding rationalises the spectroscopic data of **2**, whereby retention of solid-state composition in solution can now be postulated.

The molecular structures of the DME solvated FPhEt and FIso relatives of **2** (**5**) and **3** (**6**) are depicted in Figs. 6 and 7 with selected bond lengths listed in Table 2. While both possess an empirical composition of 1:1:1 (lithium:formamidinate:DME), the nuclearity of the complexes differs. This disrupts the lantern-like μ_2:η^1:η^1-bound $Li_2(FPhEt)_2$ conformation of **5** to yield a simple η^2-*N*,*N*′-chelated Li(FIso) monomer (**6**). The former of these bears a resemblance to the FMes analogue, $[\{Li(\mu_2{:}\eta^1{:}\eta^1\text{-}N,N'\text{-FMes})(DME)\}_2]$ [11], also a μ_2:η^1:η^1-bound dimer when coordinated by DME (herein titled **4**(4-Me)). Ignoring the structurally 'benign' 4-position methyl group, this compound serves as a model for **4**. This appears reasonable given their identical composition (by ^{1}H NMR). Thus, the addition of alkyl steric bulk to the 2- and 6-aryl positions of DME solvated lithium *N*,*N*′-di(aryl)formamidinates brings about a decrease in diazaallyl NCN angle (**4**(4-Me); 127.7(2)° [11], **5**; 125.4(2)°, **6**; 120.4(1)°), which is consistent with a transition from bridging to chelating amidinate donor. This permits a decrease in aryl:NCN plane and aryl:aryl plane torsion angles from FMes to FPhEt (**4**(4-Me); mean 66.6° and 87.2(1)° resp. [11], **5**; mean 65.5° and 84.5(1)° resp.) in spite of bigger 2- and 6-position alkyl groups, while the inherent steric buttressing necessitated by a $[Li(FIso)(DME)_2]$ dimer is too great, resulting in the formation of monomeric **6** (mean aryl:NCN plane and aryl:aryl plane torsion angles 71.9° and 75.9(1)° resp.). The overall increase in steric encumbrance from **4**(4-Me) to **5** can be gauged by the increase in angle between the N–Li–N and N–C–N planes (**4**(4-Me); 56.6(3)° [11], **5**; 63.2(2)°). This measurement derives from the "chair-like" conformations of **5** (see Fig. 6) and **4**(4-Me) [11] which, in-tandem with the related "boat", are a common feature of 8-membered metallocyclic $Li_2(NCN)_2$ species [32].

The lithium oxygen bond lengths of **4**(4-Me) [11], **5**, and **6** exhibit an increase from FMes to FPhEt (**4**(4-Me); mean 2.068 Å [11], **5**; mean 2.087 Å), and a significant decrease for monomeric **6** (mean 2.001 Å). The departure to monomeric responsible for this reduction accompanies an unusually contorted lithium coordination environment (see Fig. 7). On the basis of the steric requirements of **6** (and ^{1}H NMR data) one would expect C_{2v} symmetry about the lithium centre, as per **3** (N–Li–N plane:O–Li–O plane dihedral angle, **3**; 82.8(1)°, **6**; 67.3(1)°), however, one oxygen of the DME ligand of **6** appears twisted to one side (O(1)–Li(1)–N(2) 120.5(1)°, O(2)–Li(1)–N(2) 153.7(1)°). This may arise from the impingement of one 2,6-diisopropyl group proximal to O(1) which, in the absence of any obvious intramolecular driving force, must be a crystal packing effect.

Species **1**–**3**, **5** and **6** display bond lengths and angles that are similar to archival lithium amidinates [33] and guanidinates (see Table 2) [20,34,35]. This includes lithium to NCN donor bond lengths (mean of *N*,*N*′-chelated/bridging Li-amidinates and -guanidinates structurally characterised; 2.046 Å) [26] that are intermediate (see Table 2) between the bulky terphenyl benzamidinates of Arnold (e.g., $[Li\{\eta^1\text{-}N\text{-}(Pr^i)NC(2,6\text{-}(2,4,6\text{-}Pr^i_2C_6H_2)C_6H_3)=N(Pr^i)\}(TMEDA)]$; Li–N 1.978(8)Å) [36] and the first lithium amidinate structurally authenticated; [Li(PhNC(Ph)NPh)(PMDETA)] (PMDETA; *N*,*N*,*N*′,*N*″,*N*″-pentamethyldiethylenetriamine, Li–N 2.13 Å) [37], NCN backbone angles (for **2**, **3** and **6**) comparable to known *N*,*N*′-chelating amidinate/guanidinate species (mean 118.2°) [26], and NCN angles (compounds **1** and **5**) that are akin to those of lithiated *N*,*N*′-bridging amidinate/guanidinate species (mean 122.7°) [26]. Furthermore, unlike the benzamidinates of Arnold and coworkers [36,38], our bulky amidinates do not induce η^1-amidinate contacts with discrete C–N imino bond character for the unbound nitrogen. Instead, Li–N contacts occur in all circumstances, even **2** (bridging N(1A/B)), as is consistent with lesser encumbrance proximal to the lithium centre.

3. Sodium complexes

Worldwide, the extensive study of lithium organoamide chemistry [39,40] dwarves that of sodium species. The known alkali metal amidinates are no exception [41–43]. This takes particular relevance when one considers the increasing number of lithium and/or potassium diazaallylic species [18,19,36] where the related sodium reagent has been ignored, presumably due to its limited synthetic advantage over lithium species of lower air/moisture sensitivity compared to potassium reagents that yield halide salts of greater insolubility. However, from a structural stance, the enhanced polarity of the sodium–amide bond and the increased ionic radius of sodium (Li = 0.76 Å, Na = 1.02 Å) [44] offer increased potential for novel binding interactions. These may include rare supplementary metal-aryl contacts [45] or increased metal-*N* bridging. Furthermore, as listed above, our interest in alkali metal *N*,*N*′-di(aryl)formamidinates stems from a desire to prepare f-block

complexes via metathetical paths, thus, even though sodium halide salts are not as insoluble in ethereal solvents as their potassium congeners the suppressed reactivity of FMes [16] and related ligands [21] when metallated by potassium (see Fig. 2) make the preparation of sodium analogues of paramount synthetic importance. The incorporation of lithium halides is a prominent feature within highly polar electropositive metal organoamide [46] and amidinate/guanidinate systems [38,47–50], accordingly, THF and DME solutions of HFXyl, HFPhEt and HFIso were treated with one equivalent of sodium bis(trimethylsilyl)amide and evaluated for 'complete' metallation.

The reaction of THF or DME solutions of HFXyl, HFPhEt and HFIso with one stoichiometric equivalent of [Na{N(SiMe$_3$)$_2$}] renders the species **7**–**12** (see Fig. 1), for which the FTIR and ^{1}H NMR spectra indicate absolute transamination (N–H stretch of the parent *N*,*N*′-di(aryl)formamidine absent and, excepting **8**, fluxional ligand solution behaviour (viz. *E-syn*/*Z-anti*:*E-anti* equilibrium) [21,23] replaced by well-behaved singular ligand environments). Evaporation of the reaction medium in vacuo followed by extraction into fresh THF/DME (**8**–**10**, **12**) or hexane (**11**) permitted the isolation of clean, X-ray structure determination suitable crystals of **8**–**12**, those of **7** proving prohibitively solvent-dependent. The single crystal X-ray structure determinations of **8**–**12** were undertaken providing partial comparison for the related lithium compounds. The results of these determinations are illustrated in Figs. 8–12 (POV-RAY illustrations, thermal ellipsoids 40%) with relevant bond lengths and angles listed in Table 4. See Table 3 for a brief summary of crystallographic data.

The structures of THF complexes **8** and **9** contrast just like their lithium analogues. Compound **9** is monomeric with an η^2-*N*,*N*′-chelate donor and three terminal THF ligands occupying the remaining coordination sites. This renders a metal coordination environment that can be described as a heavily distorted trigonal

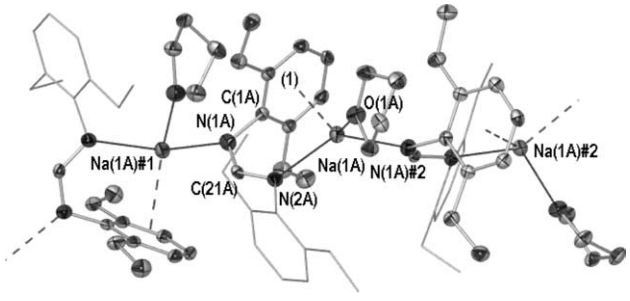

Fig. 8. X-ray crystal structure of one molecular unit of [{Na(μ_2:η^6:η^1:η^1-*Ar*,*N*,*N*′-FPhEt)(THF)}$_n$] (**8**). All hydrogen and lower occupancy disordered atoms omitted and non-coordinating aryl groups depicted as wire-frames for clarity. Symmetry transformations used to generate equivalent atoms: #1; 1−*x* + *y*, 1−*x*, *z*−1/3, #2; 1−*y*, *x*−*y*, *z* + 1/3.

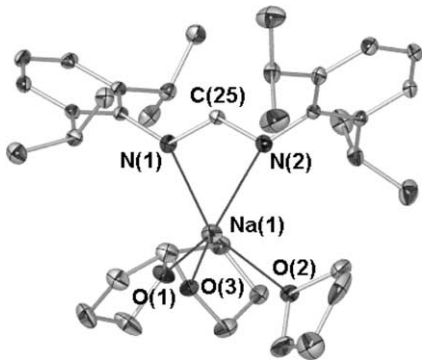

Fig. 9. X-ray crystal structure of [Na(η^2-*N*,*N*′-FIso)(THF)$_3$] (**9**). All hydrogen atoms and lower occupancy disordered atoms omitted for clarity.

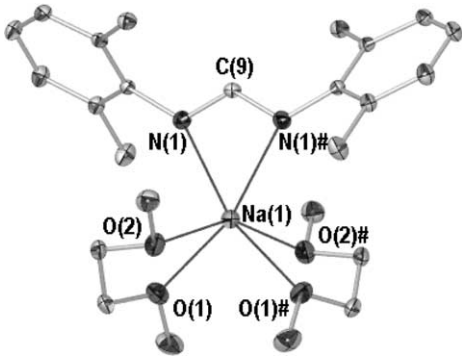

Fig. 10. X-ray crystal structure of [Na(η^2-*N*,*N*′-FXyl)(DME)$_2$] (**10**). All hydrogen atoms omitted for clarity. Symmetry transformation used to generate # atoms: −*x*, *y*, 1/2−*z*.

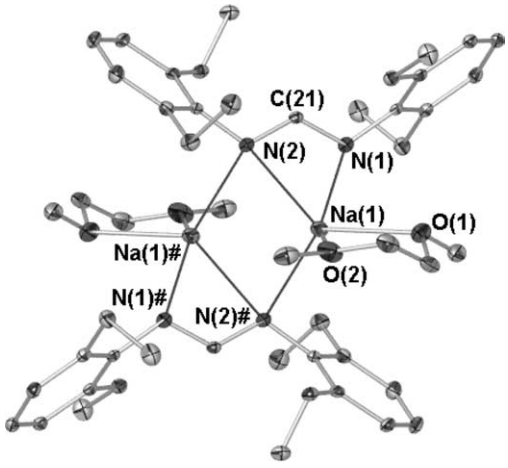

Fig. 11. X-ray crystal structure of [{Na(μ_2:η^2:η^1-*N*,*N*′-FPhEt)(DME)}$_2$] (**11**). All hydrogen atoms omitted for clarity. Symmetry transformation used to generate # atoms: 1−*x*, 1−*y*, −*z*.

bipyramid (N(2)–Na(1)–O(1) 127.1(1)°, N(1)–Na(1)–O(2) 153.6(1)°, sum of angles about Na(1) in N(2), O(1), O(3) plane 359.4°). From compounds **3** and **9** one could surmise that the positioning of two FIso

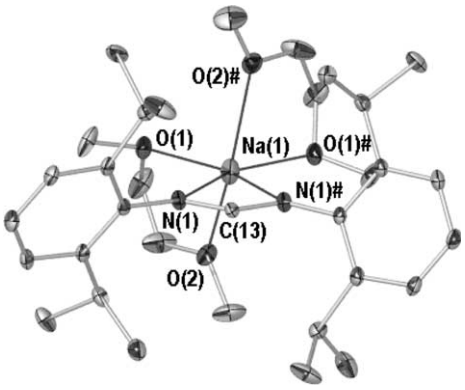

Fig. 12. X-ray crystal structure of [Na(η^2-*N*,*N*′-FIso)(DME)$_2$] (**12**). All hydrogen atoms omitted for clarity. Symmetry transformation used to generate # atoms: 1−*x*, *y*, 1/2−*z*.

ligands about lithium or sodium is not spatially viable and, hence, mononuclearity is assured. The analogous potassium system; [{K(THF)$_2$K(μ_2:η^6:η^1-*Ar*,*N*,*N*′-FIso)}$_2$] [17] (see Fig. 2) (relative six-coordinate ionic radii, K; 1.38 Å, Na; 1.02 Å, Li; 0.76 Å) [44] can achieve this due to potassium's affinity toward metal-π-aryl interactions. These negate the projection of 'all' aromatic substituents away from the NCN-bound metal. For both lithium and sodium, it appears that the *E*-*syn*/*Z*-*anti* [23] tautomerism of one or more of the *N*,*N*′-di(aryl)formamidinates of **2** and **8** provides an intermediate between NCN-bridging and NCN-chelating interactions. For compound **2**, this manifests as a singular η^1:η^1-*C*,*N*-formamidinate that bridges two lithium centres. For **8**, the lesser bulk of the FPhEt ligand relative to FIso, whilst still prohibiting discrete dimer formation, enables the *N*,*N*′-di(aryl)formamidinate to assume a *Z*-*anti* [23] tautomeric conformation and participate as a bridge in an infinite Na(FPhEt)(THF) polymer vide infra. (Note: in terms of the Carr–Ingold–Prelog nomenclature employed, when sodium is coordinated *E*-*syn* becomes *Z*-*anti* and vice versa due to the modified priority sequence of the groups attached vis-à-vis lithium species, e.g., **2**) [23]. The *N*,*N*′-di(aryl)formamidinate coordination is supplemented by a terminal THF donor and a *N*-interaction from an adjoining unit, thereby furnishing sodium with a near tetrahedral environment if one considers the coordinated arene as a single point donor (three molecular units within the asymmetric unit, mean arene centroid–Na–*inter*-'monomer' N; 109.3°, mean O–Na–*intra*-'monomer' N; 100.9°). As the diazaallyl fragments of all three 'monomer' units in the asymmetric unit of **8** lack a consistent N–C–N bond order, i.e., the backbone C–N bond lengths for the bridging and non-bridging nitrogen atoms depict *intra*-ligand discrepancies of 0.002 Å (molecule A) to 0.020 Å (molecule B, these remain suggestive of significant charge delocalisation across the NCN-unit, viz., HFPhEt C–N/C=N discrepancy; 0.077 Å) [21], the tautomerism of the μ_2:η^6:η^1:η^1-*Ar*,*N*,*N*′-FPhEt ligand could only be extrapolated through comparison of the *intra*- and *inter*-'monomer' unit Na–N bond lengths. In all three instances (molecules A–C), the *inter*-bond length is shorter than that of the *intra*-, inferring Na(1)–N(2) is the metal amide bond. This discrepancy varies from 0.029 Å (molecule A) to 0.056 Å (molecule B) suggesting the ligands therein can be tentatively assigned as *Z*-*anti* tautomers. However, caution must be taken as this contrast in lengths may derive from the

Table 3
Summary of crystal data for sodium compounds **8**–**12**

	[{Na(μ_2:η^6:η^1:η^1-*Ar*,*N*,*N*′-FPhEt)(THF)}$_n$] (**8**)	[Na(η^2-*N*,*N*′-FIso)(THF)$_3$] (**9**)	[Na(η^2-*N*,*N*′-FXyl)(DME)$_2$] (**10**)	[Na(μ_2:η^2:η^1-*N*,*N*′-FPhEt)(DME)$_2$] (**11**)	[Na(η^2-*N*,*N*′-FIso)(DME)$_2$] (**12**)
Mol. formula	$C_{25}H_{35}N_2O_1Na_1$	$C_{37}H_{59}N_2O_3Na_1$	$C_{25}H_{39}N_2O_4Na_1$	$C_{25}H_{37}N_2O_2Na_1$	$C_{33}H_{55}N_2O_4Na_1$
Mol. weight	1207.62	602.85	227.29	420.56	283.39
Temperature (K)	123(2)	123(2)	123(2)	123(2)	123(2)
Space group	$P3_1$	$P2_12_12_1$	*C*2/*c*	$P2_1/n$	*C*2/*c*
a (Å)	19.3628(4)	10.778(2)	22.185(4)	11.3502(3)	20.108(4)
b (Å)	19.3628(4)	17.479(4)	9.765(2)	11.7962(4)	8.8267(18)
c (Å)	16.2509(5)	19.142(4)	15.716(3)	18.5305(6)	20.830(4)
α (°)	90	90	90	90	90
β (°)	90	90	128.66(3)	102.997(2)	112.85(3)
γ (°)	120	90	90	90	90
Volume (Å^3)	5276.5(15)	3606.1(13)	2658.6(9)	2417.5(1)	3407.0(12)
Z	9	4	4	4	4
D_c (g cm^{-3})	1.140	1.110	1.136	1.156	1.105
μ (mm^{-1})	0.085	0.079	0.090	0.088	0.082
Reflections collected	62,778	41,155	5319	22,642	11,060
Unique reflections	16,521	8920	3178	5777	3950
Parameters varied	817	406	150	277	188
R_{int}	0.1234	0.0848	0.0459	0.0573	0.0854
R_1	0.0778	0.0582	0.0468	0.0594	0.0773
wR_2	0.1199	0.1357	0.0893	0.1159	0.1820

Table 4
Selected bond lengths (Å) and angles (°) for sodium compounds **8**–**12**

Compound ***8***[a]					
Na(1A)–N(1A)#2	2.340(3)	Na(1A)–C(4A)	3.368(4)	C(1A)–C(2A)	1.403(5)
Na(1A)–N(2A)	2.369(3)	Na(1A)–C(5A)	3.292(4)	C(1A)–C(6A)	1.414(5)
Na(1A)–(1)[b]	2.79(1)	Na(1A)–C(6A)	3.041(4)	C(2A)–C(3A)	1.392(5)
Na(1A)–O(1A)	2.300(3)	N(1A)–C(1A)	1.419(5)	C(5A)–C(6A)	1.397(5)
Na(1A)–C(1A)	2.852(4)	N(1A)–C(21A)	1.315(5)	C(3A)–C(4A)	1.377(6)
Na(1A)–C(2A)	2.956(4)	N(2A)–C(21A)	1.317(5)	C(4A)–C(5A)	1.373(6)
Na(1A)–C(3A)	3.206(4)				
N(1A)#2–Na(1A)–N(2A)	134.2(1)	N(2A)–Na(1A)–O(1A)	103.5(1)	C(1A)–N(1A)–C(21A)	115.5(3)
N(1A)#2–Na(1A)–(1)[b]	108.8(3)	(1)[b] -Na(1A)–O(1A)	129.9(3)	Na(1A)–N(2A)–C(21A)	123.4(3)
N(1A)#2–Na(1A)–O(1A)	94.1(1)	Na(1A)#1–N(1A)–C(1A)	125.5(2)	N(1A)–C(21A)–N(2A)	128.8(3)
N(2A)–Na(1A)–(1)[b]	91.8(3)	Na(1A)#1–N(1A)–C(21A)	117.5(2)		
Compound ***9***					
Na(1)–N(1)	2.406(2)	Na(1)–O(2)	2.347(2)	N(1)–C(25)	1.320(3)
Na(1)–N(2)	2.457(2)	Na(1)–O(3)	2.376(2)	N(2)–C(25)	1.313(3)
Na(1)–O(1)	2.351(2)				
N(1)–Na(1)–N(2)	56.6(1)	N(2)–Na(1)–O(1)	127.1(1)	O(1)–Na(1)–O(3)	107.5(1)
N(1)–Na(1)–O(1)	108.4(1)	N(2)–Na(1)–O(2)	97.6(1)	O(2)–Na(1)–O(3)	87.8(1)
N(1)–Na(1)–O(2)	153.6(1)	N(2)–Na(1)–O(3)	124.9(1)	N(1)–C(25)–N(2)	122.1(2)
N(1)–Na(1)–O(3)	102.5(1)	O(1)–Na(1)–O(2)	91.1(1)		
Compound ***10***[c]					
Na(1)–N(1)	2.426(1)	Na(1)–O(2)	2.436(2)	N(1)–C(9)	1.318(2)
Na(1)–O(1)	2.365(1)				
N(1)–Na(1)–N(1)#	56.6(1)	N(1)–Na(1)–O(2)#	112.0(1)	O(1)–Na(1)–O(2)#	88.9(1)
N(1)–Na(1)–O(1)	104.4(1)	O(1)–Na(1)–O(2)	70.7(1)	O(2)–Na(1)–O(2)#	149.9(1)
N(1)–Na(1)–O(2)	94.8(1)	O(1)–Na(1)–O(1)#	94.9(6)	N(1)–C(9)–N(1)#	121.6(2)
N(1)–Na(1)–O(1)#	160.5(1)				
Compound ***11***[d]					
Na(1)–N(1)	2.394(2)	Na(1)–O(1)	2.370(2)	N(1)–C(21)	1.311(2)
Na(1)–N(1)#	2.476(2)	Na(1)–O(2)	2.376(2)	N(2)–C(21)	1.331(2)
Na(1)–N(2)	2.617(2)	Na(1)···Na(1)#	3.147(1)		
N(2)–Na(1)–N(2)#	103.7(1)	N(2)#–Na(1)–O(2)	93.7(1)	Na(1)–N(2)–Na(1)#	76.3(1)
N(1)–Na(1)–N(2)	55.2(1)	N(2)#–Na(1)–O(1)	120.8(1)	Na(1)–N(2)–C(21)	83.3(1)
N(2)–Na(1)–O(2)	118.6(1)	N(1)–Na(1)–O(2)	132.7(1)	Na(1)#–N(2)–C(21)	140.2(1)
N(2)–Na(1)–O(1)	134.4(1)	N(1)–Na(1)–O(1)	85.0(1)	Na(1)–N(1)–C(21)	93.2(1)
N(2)#–Na(1)–N(1)	133.5(1)	O(1)–Na(1)–O(2)	70.6(1)	N(1)–C(21)–N(2)	123.6(2)
Compound ***12***[e]					
Na(1)–N(1)	2.411(3)	Na(1)–O(2)	2.438(3)	N(1)–C(13)	1.316(3)
Na(1)–O(1)	2.388(2)				
N(1)–Na(1)–N(1)#	57.0(1)	N(1)–Na(1)–O(2)#	114.1(1)	O(1)–Na(1)–O(2)#	84.3(1)
N(1)–Na(1)–O(1)	99.9(1)	O(1)–Na(1)–O(2)	69.3(1)	O(2)–Na(1)–O(2)#	137.2(1)
N(1)–Na(1)–O(2)	103.6(1)	O(1)–Na(1)–O(1)#	103.3(1)	N(1)–C(13)–N(1)#	121.7(4)
N(1)–Na(1)–O(1)#	156.8(1)				

[a] Three molecular units in the asymmetric unit. Due to similar metrical parameters only molecule "A" listed. Symmetry transformations used to generate equivalent atoms: #1; $1-x+y$, $1-x$, $z-1/3$, #2; $1-y$, $x-y$, $z+1/3$.
[b] Atoms C(1A)–C(6A) used to derive the coordinated 2,6-$Et_2C_6H_2$ centroid "(1)".
[c] Symmetry transformations used to generate # atoms: $-x$, y, $1/2-z$.
[d] Symmetry transformations used to generate # atoms: $1-x$, $1-y$, $-z$.
[e] Symmetry transformations used to generate # atoms: $1-x$, y, $1/2-z$.

η^6:η^1-Ar,*N*-donor motif, which exerts considerable strain for **8** relative to the η^1-aryl binding of **2** about lithium and the η^6-aryl binding of $[\{K(THF)_2K(\mu_2{:}\eta^6{:}\eta^1{:}\eta^1\text{-}Ar,N,N'\text{-FIso})_2]$ about potassium [17]. This is borne out by the decreased proximity of the *para*- and *meta*-position carbons of the arene donor, e.g., C(4A) and C(3A)/C(5A), to the metal by ca. 0.25 Å relative to the *ipso*- and *ortho*-carbons, e.g., C(1A) and C(2A)/C(6A) (see Table 4). Nonetheless, these contacts are still within the accepted boundary of Na–C arene [27,45,51] such as those listed for Robinson's 'gallyne'; $[Na]_2[Ga_2(2,6\text{-}Trip_2C_6H_3)_2]$ (<3.397 Å) [1] and the solvent free triptylthiolates (<3.661 Å) of Ruhlandt-Senge [52]. In addition, unlike the η^1-aryl

binding of **2** (see Table 2), the increased proximity of the sodium to the *ipso*- and *ortho*-carbons has a noticeable effect on the bond-lengths around the arene donor. For molecule A this manifests as a ca. 0.035 Å extension of the C(1A) (*ipso*-carbon) to C(2A)/C(6A) (*ortho*-carbons) bond lengths relative to the C(4A) (*para*-carbon) to C(3A)/C(5A) (*meta*-carbons) bond lengths (see Table 4).

The ^{1}H NMR spectrum resonances attributable to the ethyl groups of **8**, like those of **2** but not the methyls of **7**, are suggestive of asymmetric amidinate geometry in solution (CH_3 resonances broadened triplets at 1.17 and 1.39 ppm, CH_2 resonances broadened quadruplets 2.47 and 2.84 ppm; 3:3:2:2 ratio). As both **2** and **8** freely exhibit a ''solid-state'' consistent nature on this basis, i.e. ^{1}H NMR data indicate retention of solid-state binding modes, it is reasonable to speculate that the solid-state composition of **7** does not exhibit sodium–arene interactions or an asymmetric binding mode. Furthermore, the extreme solvent dependency of **7** suggests its molecular composition incorporates less THF than the overall empirical value (^{1}H NMR; 2.0 THF molecules per Na(FXyl)). In itself, one could conject that this necessitates FXyl-bridging interactions, perhaps akin to those observed for **11** (vide infra). Finally, the relative orientations of the aromatic rings in **8** and **9** generate mean torsion angles of 60.1° and 72.0(1)°, which in the arene-donor cases of **8** are also accompanied by near perpendicular placement of the aromatic rings to the NCN backbone (mean aryl donor plane: NCN; 87.8°, non-donor; 70.2°). A similar disposition for the FIso ligand of **9** is not necessary on the basis of its monomeric composition, this 'frees' the 2,6-diisopropylphenyl groups rendering NCN:aryl plane dihedral angles of 63.4(2)° and 69.4(2)°, again suggesting η^2-*N*,*N*′-coordination diminishes congestion about the metal ligand frame.

The molecular structures of DME species **10**–**12** are depicted in Figs. 10–12 (POV-RAY illustrations, 40% thermal ellipsoids). All relevant bond lengths and angles are given in Table 4. Unlike the related THF species, but as per their lithium analogues, the steric constraints of DME reduce the breadth of ligand binding observed relative to the THF examples. This can be seen in Figs. 10 and 12, which exhibit singular η^2-*N*,*N*′-donors and two chelated DME donors. The apparent structural discrepancies between **10** and **12** are the Na–N and Na–O bond lengths (**10**; Na–N 2.426(2) Å, mean Na–O 2.401 Å, **12**; Na–N 2.411(3) Å, mean Na–O 2.413 Å) and the relative positioning of the arene planes to the *N*,*N*′-di(aryl)formamidinate frame (NCN : aryl torsion angle **10**; 50.1(1)°, **11**; 67.6(1)°). This placement incurs moderately smaller DME bite angles for **12** owing to buttressing of the methoxy groups with the 2,6-diisopropylphenyl substituents (**10**; 70.7(1)°, **12**; 69.3(1)°). Overall, the sodium coordination geometries of both can be considered as heavily distended octahedra (*cis* and *trans* O–Na–O angles excluding DME bite, **10**; 88.9(1)°/94.9(1)° and 149.9(1)°, **12**; 84.3(1)°/103.3(1) and 137.2(1)°, respectively). For compound **11** (Fig. 11), repeated failure to isolate crystalline samples suitable for structure determination from DME led to recrystallisation from hexane. This gave the species illustrated, wherein extraction into hexane resulted in the loss of one DME (see compounds **10** and **12**). The ^{1}H NMR of the vacuum dried product from treatment of HFPhEt with sodium bis(trimethylsilyl)amide in DME exhibits the expected composition based on **10** and **12** (1 FPhEt:2 DME), and thus concentration of hexane solutions of **11** in vacuo must permit solvent loss despite the increased boiling point of DME relative to hexane. Compound **11** is a μ_2:η^2:η^1-bound Na(FPhEt) dimer that resembles the FTolP complex [{Na(μ_2:η^2:η^1-*N*,*N*′-FTolP)(DME)}$_2$] [8]. This also exhibits a μ_2:η^2:η^1-dimeric composition that in turn is reminiscent of the first alkali metal *N*,*N*′-di(aryl)formamidinate complex structurally authenticated; [{Li(μ_2:η^2:η^1-*N*,*N*′-FTolP)(Et_2O)}$_2$] [24]. As expected, the internal chelate Na–N distance of the bridging nitrogen (Na(1)–N(2) 2.617(2) Å) is somewhat longer than the other Na–N contacts (Na(1)–N(1) 2.394(2) Å, Na(1)–N(2)# 2.476(2) Å), and the sodium···sodium distance is greater than that of its FTolP relative (**11**; 3.147(2) Å, FTolP; 3.080(2)Å) [8]. Predictably, the entire dimer frame is far more strained. This leads to considerable twisting of the aromatic planes of **11** relative to the NCN backbone (60.3(1)° and 67.8(2)°, FTolP example 27.3(3)° and 30.4(2)°) [8].

4. Experimental

The *N*,*N*′-di(aryl)formamidinate ligand precursors *N*,*N*′-di(2,6-dimethylphenyl)-, *N*,*N*′-di(2,6-diethylphenyl) and *N*,*N*′-di(2,6-diisopropylphenyl)formamidine, HFXyl, HFPhEt and HFIso, respectively, were synthesised according to a modified published procedure [53]. *n*-Butyl lithium (1.6 M in hexanes) and sodium bis(trimethylsilyl)amide (1.0 M in THF) were purchased from Aldrich. Tetrahydrofuran (THF) and hexane were dried over sodium, freshly distilled from sodium benzophenone ketyl and freeze–thaw degassed prior to use. 1,2-Dimethoxyethane (DME) was dried over sodium wire and freshly distilled from sodium prior to use. All manipulations were performed using conventional Schlenk or glovebox techniques under an atmosphere of high purity dinitrogen in flame-dried glassware. Infrared spectra were recorded as Nujol mulls using sodium chloride plates on a Nicolet Nexus FTIR spectrophotometer. ^{1}H NMR spectra were recorded at 300.13 MHz and ^{13}C NMR spectra were recorded at 75.46 MHz using a Bruker DPX 300 spectrometer, and chemical shifts were referenced to the residual ^{1}H or ^{13}C

resonances of the *deutero*-benzene solvent. Melting points were determined in sealed glass capillaries under dinitrogen and are uncorrected.

4.1. General procedure

n-Butyl lithium (1.00 cm^3, 1.6 mmol) or sodium bis(trimethylsilyl)amide (1.6 cm^3, 1.6 mmol) was added dropwise to a stirred solution of *N*,*N*′-di(aryl)formamidine (HFXyl; 0.40 g, 1.59 mmol, HFPhEt; 0.49 g, 1.59 mmol, HFIso; 0.58 g, 1.59 mmol) in THF (compounds **1** and **7**; 40 cm^3, compounds **2** and **8**; 35 cm^3, compounds **3** and **9**; 20 cm^3) or DME (compounds **4** and **10**; 30 cm^3, compounds **5**, **6**, **11** and **12**; 20 cm^3) at ambient temperature. The resulting solution, which ranged from colourless to light yellow in appearance, was then stirred overnight. Filtration followed by removal of volatiles under reduced pressure rendered a colourless powder devoid of FTIR absorbances and ^{1}H NMR resonances attributable to the parent *N*,*N*′-di(aryl)formamidine. Relevant details for each compound are as follows:

4.2. [$Li_2(\mu_2$:η^1:η^1-*N,N′-FXyl*)$_2(\mu_2$-*THF*)(*THF*)$_2$] (**1**)

Extraction into fresh tetrahydrofuran (10 cm^3) followed by concentration in vacuo (ca. 4 cm^3) gave large light yellow irregular prisms of **1** after standing at ambient temperature over several days (0.40 g, 69%), m.p. 236 °C. ^{1}H NMR (C_6D_6, 300 K): δ 1.39 (m, 12H, CH_2, THF), 2.35 (s, 24H, CH_3), 3.40 (m, 12H, OCH_2, THF), 6.89 (m, 4H, Ar-*p*-*H*), 7.04 (m, 8H, Ar-*m*-*H*), 7.87 (br s, 2H, NC(*H*)N). ^{13}C NMR (C_6D_6, 300 K): δ 20.4 (s, C_3), 25.9 (s, C_2, THF), 68.3 (s, O*C*H$_2$, THF), 122.2, 128.9, 132.3, 136.3 (s, Ar-*C*), 167.2 (s, N*C*(H)N). IR (Nujol)/cm^{-1}: 1687 (br m), 1539 (m), 1484 (sh m), 1350 (m), 1324 (sh s), 1272 (br m), 1210 (m), 1145 (w), 1087 (m), 1038(m), 1107 (m), 862 (s), 842 (br m).

4.3. [*Li(THF)*$_3$(μ_2:η^1:η^1:η^1-*N,C,N′-FPhEt*)*Li*(η^2-*N,N′-FPhEt*)]·*THF* (**2**)

Extraction into fresh tetrahydrofuran (10 cm^3) followed by concentration in vacuo (ca. 3 cm^3) gave large colourless irregular prismatic crystals after placement at −10 °C overnight (0.48 g, 66%), m.p. 134 °C (dec.). ^{1}H NMR (C_6D_6, 300 K): δ 1.33 (br t, 6H, CH_2CH_3, μ_2:η^1:η^1:η^1-*N,C,N′*-FPhEt), 1.36 (br t, 6H, CH_2CH_3, μ_2:η^1:η^1:η^1-*N,C,N′*-FPhEt), 1.39 (br t, 12H, CH_2CH_3, η^2-*N,N′*-FPhEt), 1.53 (m, 16H, CH_2, THF), 2.88–2.92 (br m, 16H, *CH*$_2$ all FPhEt), 3.51 (m, 16H, OCH_2, THF), 7.09 (m, 2H, Ar-*H*), 7.17 (m, 6H, Ar-*H*), 7.23 (m, 4H, Ar-*H*), 7.87 (br s, 2H, NC(*H*)N). ^{13}C NMR (C_6D_6, 300 K): δ 14.3 (s, CH_2CH_3), 15.6 (s, CH_2CH_3), 15.7 (s, CH_2CH_3), 24.2 (s, *C*H$_2$, FPhEt or THF), 24.4 (s, *C*H$_2$, FPhEt or THF) 25.6 (s, *C*H$_2$, FPhEt or THF), 68.3 (s, O*C*H$_2$, THF), 121.1, 123.2, 124.6, 125.0, 136.9, 138.0, 143.7, 149.0 (s, Ar-*C*), 166.1 (s, N*C*(H)N). IR (Nujol)/cm^{-1}: 1660 (sh m), 1543 (m), 1358 (m), 1332, (s), 1281 (m), 1203 (m), 1183 (m), 1088 (m), 1042(m), 1001 (m), 857 (m), 842 (m).

4.4. [*Li*(η^2-*N,N′-FIso*)(*THF*)$_2$] (**3**)

Extraction into fresh tetrahydrofuran (10 cm^3) followed by concentration in vacuo (ca. 5 cm^3) gave the title compound as large colourless elongated blocks in three separate batches after placement at −30 °C over several days (total 0.67 g, 81%), m.p. 259 °C. ^{1}H NMR (C_6D_6, 300 K): δ 1.31 (d, 24H, CH(CH_3)$_2$, $^3J_{HH}$ 6.9 Hz), 1.38 (m, 8H, CH_2, THF), 3.41 (m, 8H, OCH_2, THF), 3.76 (h, 4H, CH(CH$_3$)$_2$, $^3J_{HH}$ 6.9 Hz), 7.13 (m, 2H, Ar-*p*-*H*), 7.18 (m, 4H, Ar-*m*-*H*), 7.89 (br s, 1H, NC(*H*)N). ^{13}C NMR (C_6D_6, 300 K): δ 24.8 (s, CH(*C*H$_3$)$_2$), 25.9 (s, *C*H$_2$, THF), 28.6 (s, *C*H(CH$_3$)$_2$), 66.3 (s, O*C*$_2$, THF), 123.8, 128.5, 132.3, 143.5 (s, Ar-*C*), 161.3 (s, N*C*(H)N). IR (Nujol)/cm^{-1}: 1607 (sh m), 1554 (m), 1538 (s), 1366 (m), 1302, (s), 1289 (m), 1198 (m), 1114 (m), 1087 (m), 1042(m), 993 (sh m), 872 (s), 840 (m), 803 (m), 760 (s).

4.5. [*Li(FXyl)(DME)*] (**4**)

Extraction into fresh 1,2-dimethoxyethane (10 cm^3) followed by concentration in vacuo (ca. 5 cm^3) gave **4** as highly solvent dependent blocks after cooling to −10 °C overnight. These were isolated by filtration, dried under dynamic nitrogen for 24 h and characterised thereafter (0.37 g, 67%), m.p. >350 °C. ^{1}H NMR (C_6D_6, 300 K): δ 2.34 (s, 12H, CH_3), 2.91 (s, 4H, OCH_2, DME), 2.92 (s, 6H, OCH_3, DME), 6.92 (m, 2H, Ar-*p*-*H*), 7.10 (m, 4H, Ar-*m*-*H*), 7.74 (br s, 2H, NC(*H*)N). ^{13}C NMR (C_6D_6, 300 K): δ 20.3 (s, *C*H$_3$), 59.1 (s, O*C*H$_3$, DME), 71.4 (s, O*C*H$_2$, DME), 121.8, 128.7, 132.3, 142.4 (s, Ar-*C*), 157.3 (s, N*C*(H)N). IR (Nujol)/cm^{-1}: 1663 (m), 1602 (m), 1537 (m), 1383 (m), 1316 (m), 1253 (s), 1202 (sh m), 1108 (br s), 1035 (s), 944 (m), 863 (m), 758 (m).

4.6. [{*Li*(μ_2:η^1:η^1-*N,N′-FPhEt*)(*DME*)}$_2$] (**5**)

Dissolution of the colourless powdered material into 1,2-dimethoxyethane (10 cm^3) gave a yellow solution that was concentrated in vacuo (ca. 6 cm^3) and filtered. Placement at −15 °C rendered colourless cubic crystals (0.30 g, 47%), m.p. >350 °C. ^{1}H NMR (C_6D_6, 300 K): δ 1.09 (m, 12H, CH_2CH_3), 2.63 (m, 8H, CH_2CH$_3$), 2.68 (s, 8H, OCH_2, DME), 2.78 (s, 12H, OCH_3, DME), 6.88–6.97 (m, 6H, Ar-*H*), 7.49 (br s, 1H, NC(*H*)N). ^{13}C NMR (C_6D_6): δ 15.6 (s, CH_2CH_3), 25.9 (s, *C*H$_2$CH$_3$), 58.9 (s, O*C*H$_3$, DME), 70.9 (O*C*H$_2$,

DME), 122.7, 126.1, 138.5, 149.9 (s, Ar-*C*), 168.0 (s, N*C*(H)N). IR (Nujol)/cm^{-1}: 1661 (m), 1596 (br s), 1546 (br s), 1189 (s), 1029 (s), 918 (sh s), 963 (sh s), 803 (sh s), 673 (sh s).

4.7. [Li(η^2-N,N′-FIso)(DME)] (6)

Extraction into fresh 1,2-dimethoxyethane (10 cm^3) followed by immediate filtration yielded colourless prisms upon standing. These were collected by filtration and washed with cold (ca. 0 °C) hexane (2 × 2 cm^3) (0.30 g, 0.41 g), m.p. 337 °C (dec.). ^{1}H NMR (C_6D_6, 300 K): δ 1.39 (d, 12H, CH(CH_3)$_2$, $^3J_{HH}$ 6.9 Hz), 2.82 (s, 4H, OCH_2, DME), 3.06 (s, 6H, OCH_3, DME), 3.81 (h, 4H, CH(CH$_3$)$_2$), 7.16–7.22 (m, 2H, Ar-*H*), 7.28–7.31 (m, 4H, Ar-*H*), 8.02 (br s, 1H, NC(*H*)N). ^{13}C NMR (C_6D_6, 300 K): δ 23.1 (s, CH(*C*H$_3$)$_2$), 57.7 (s, O*C*H$_3$, DME), 69.0 (s, O*C*H$_2$, DME), 120.8, 121.8, 141.4, 148.3 (Ar-*C*), 164.5 (s, NC(*H*)N). IR (Nujol) ν/cm^{-1}: 1602 (sh m), 1554 (m), 1538 (s), 1366 (m), 1302, (s), 1289 (m), 1198 (m), 1114 (m), 1087 (m), 1042 (m), 993 (sh m), 872 (s), 840 (m), 803 (m), 760 (s).

4.8. [Na(FXyl)(THF)$_2$] (7)

Extraction into fresh tetrahydrofuran (15 cm^3) and concentration in vacuo (ca. 10 cm^3) gave a microcrystalline material upon standing that was unsuitable for X-ray structure determination. Further filtration followed by slow-cooling to 0 °C in an acetone bath yielded small colourless prisms that underwent solvent loss upon warming to room temperature (0.22 g, 33%), solvent loss ca. 15 °C, residual material m.p. 158 °C. Cooled (sub 15 °C) material used for characterisation. ^{1}H NMR (C_6D_6, 300 K): δ 2.26 (s, 12H, CH_3), 1.57 (m, 8H, CH_2, THF), 3.57 (m, 8H, OCH_2, THF), 6.99 (m, 2H, Ar-*p*-*H*), 7.11 (m, 4H, Ar-*m*-*H*), 7.67 (br s, 1H, NC(*H*)N). ^{13}C NMR (C_6D_6, 300 K): δ 20.6 (s, *C*H$_3$), 24.6 (s, *C*H$_2$, THF), 67.9 (s, O*C*H$_2$, THF), 123.6, 127.2, 131.8, 144.4 (s, Ar-*C*), 156.9 (s, N*C*(H)N). IR (Nujol)/cm^{-1}: 1645 (m), 1600 (m), 1567 (m), 1345 (br m), 1298 (m), 1212 (m), 1180 (m), 1087 (br s), 1035 (w), 990 (sh m), 867 (m), 837 (m), 802 (m), 772 (m).

4.9. [{Na(μ_2:η^6:η^1:η^1-Ar,N,N′-FPhEt)(THF)}$_n$] (8)

Extraction into fresh tetrahydrofuran (10 cm^3) followed by filtration gave highly air-sensitive small blocks after cooling to −10 °C (0.29 g, 45%), m.p. 83 °C. ^{1}H NMR (C_6 D_6, 300 K): δ 1.17 (br t, 6H, CH$_2$CH_3), 1.39 (br t, 6H, CH$_2$CH_3), 1.52 (m, 4H, CH_2, THF), 2.47 (br q, 4H, CH_2CH$_3$), 2.84 (br q, 4H, CH_2CH$_3$), 3.58 (m, 4H, OCH_2), 7.06 (m, 1H, Ar-*H*), 7.24 (m, 3H, Ar-*H*), 7.38 (m, 2H, Ar-*H*), 7.63 (br s, 1H, NC(*H*)N). ^{13}C NMR (C_6D_6, 300 K): δ 13.0 (s, CH$_2$*C*H$_3$), 14.0 (s, CH$_2$*C* H$_3$), 23.3 (s, *C*H$_2$, FPhEt or THF), 24.1 (s, *C*H$_2$, FPhEt or THF), 24.3 (s, *C*H$_2$, FPhEt or THF), 66.6 (s, O*C*H$_2$, THF), 121.5, 121.8, 125.0, 125.5, 136.8, 137.1, 146.7 (s, Ar-*C*), 161.1 (s, N*C*(H)N). IR (Nujol)/cm^{-1}: 1665 (m), 1601 (m), 1564 (m), 1316 (s), 1289 (m), 1189 (br m), 1111 (s), 1067 (m), 993 (m), 870 (m), 803 (m), 761 (m), 720 (w).

4.10. [Na(η^2-N,N′-FIso)(THF)$_3$] (9)

Extraction into tetrahydrofuran (ca. 5 cm^3), filtration and standing at room temperature over a period of several days yielded the title compound as large hexagonal prisms (0.85, 89%), m.p. 256 °C. ^{1}H NMR (C_6D_6, 300 K): δ 1.39 (d, 24H, CH(CH_3)$_2$, $^3J_{HH}$ 6.8 Hz), 1.50 (m, 12H, CH_2, THF), 3.58 (m, 12H, OCH_2, THF), 3.88 (s, 4H, CH(CH$_3$)$_2$, $^3J_{HH}$ 6.8 Hz), 7.12 (m, 2H, Ar-*p*-*H*), 7.27 (m, 4H, Ar-*m*-*H*), 7.90 (br s, 1H, NC(*H*)N). ^{13}C NMR (C_6D_6, 300 K): δ 25.4 (s, *C*H$_2$, thf), 26.6 (s, C*C*H$_3$), 31.1 (s, *C*H(CH$_3$)$_2$), 68.9 (s, O*C*H$_2$), 121.9, 123.9, 143.4, 152.4 (s, Ar-*C*), 164.9 (s, N*C*(H)N). IR (Nujol)/cm^{-1}: 1667 (sh m), 1594 (sh m), 1538 (s), 1317 (s), 1255 (sh s), 1236 (m), 1186 (m), 1158 (w), 1143 (w), 1099 (m), 1048 (s), 992 (m), 934 (m), 920 (m), 822 (w), 807 (m), 778 (m), 757 (m), 669 (w).

4.11. [Na(η^2-N,N′-FXyl)(DME)$_2$] (10)

Extraction in fresh 1,2-dimethoxyethane (10 cm^3) followed by concentration in vacuo (ca. 2 cm^3) gave colourless needles of **10** (0.45 g, 63%), m.p. 62 °C (dec.). ^{1}H NMR (C_6D_6, 300 K): δ 2.36 (s, 12H, CH_3), 3.03 (s, 6H, OCH_3, DME), 3.11 (s, 4H, OCH_2, DME), 6.98 (m, 2H, Ar-*p*-*H*), 7.12 (m, 4H, Ar-*m*-H), 7.67 (br s, 1H, NC(*H*)N). ^{13}C NMR (C_6D_6, 300 K): δ 18.4 (s, *C*$_3$), 57.4 (s, O*C*H$_3$, DME), 70.5 (s, O*C*H$_2$, DME), 120.6, 125.0, 130.6, 144.9 (s, Ar-*C*), 159.3 (s, N*C*(H)N). IR (Nujol)/cm^{-1}: 1651 (m), 1590 (m), 1538 (m), 1317 (m), 1248 (m), 1199 (sh m), 1114 (br s), 1032 (s), 944 (m), 859 (m), 758 (sh m), 666 (w).

4.12. [{Na(μ_2:η^2:η^1-FPhEt)(DME)}$_2$] (11)

Extraction into hexane (25 cm^3) followed by filtration and repeated concentration under reduced pressure (to ca. 9 cm^3) rendered colourless prisms of **11** (0.28 g, 42%), m.p. 270 °C. ^{1}H NMR (C_6D_6, 300 K): δ 1.24 (t, 24H, CH$_2$CH_3, $^3J_{HH}$ 7.5 Hz), 2.70 (q, 16H, CH_2CH$_3$, $^3J_{HH}$), 2.98 (s, 8H, OCH_2, DME), 3.02 (s, 12H, OCH_3, DME), 6.90 (m, 4H, Ar-*p*-*H*), 7.08 (m, 8H, Ar-*m*-H), 7.34(br s, 2H, NC(*H*)N). ^{13}C NMR (C_6D_6, 300 K): δ 13.6 (s, CH$_2$*C*H$_3$), 24.0 (s, *C*H$_2$CH $_3$), 57.4 (s, O*C*H$_3$, DME), 70.0 (s, O*C*H$_2$), 122.3, 125.4, 130.6, 143.8 (s, Ar-*C*), 161.8 (s, N*C*(H)N). IR (Nujol)/cm^{-1}: 1649 (sh m), 1587 (m), 1537 (s), 1375 (sh m), 1330 (m), 1254 (m), 1189 (sh m), 1102 (m), 1032 (m), 920 (sh w), 808 (m), 751 (s), 667 (w).

4.13. [Na(η²-N,N′-FIso)(DME)₂] (12)

Extraction into fresh 1,2-dimethoxyethane (10 cm^3) followed by standing for several days yielded **12** as colourless hexagonal prismatic rods (0.58 g, 64%), m.p. 118 °C. ^{1}H NMR (C_6D_6, 300 K): δ 1.41 (d, 24H, CH(CH_3)$_2$, $^3J_{HH}$ 6.5 Hz), 2.97 (2 × s, 20H, OCH_2 and OCH_3, DME), 3.80 (h, 4H, $CH(CH_3)_2$, $^3J_{HH}$ 6.5 Hz), 7.13 (m, 2H, Ar-*p*-*H*), 7.25 (m, 4H, Ar-*m*-H), 7.85 (br s, 1H, NC(*H*)N). ^{13}C NMR (C_6D_6, 300 K): δ 23.3 (s, CH(CH_3)$_2$), 26.8 (s, $CH(CH_3)_2$), 57.4 (s, OCH_3, DME), 70.0 (s, OCH_2, DME), 120.3, 121.7, 127.0, 141.3 (s, Ar-*C*), 162.7 (s, N*C*(H)N). IR (Nujol)/cm^{-1}: 1661 (m), 1589 (m), 1539 (s), 1350 (m), 1322 (m), 1294 (m), 1244 (m) 1194 (sh m), 1111 (br s), 1067 (m), 1022 (sh m), 983 (sh w), 933 (sh m), 856 (m), 794 (w), 756 (sh s).

5. X-ray crystallography

Crystalline samples of compounds **1**–**3**, **5**, **6**, **8**–**12** were mounted on glass fibres, in viscous hydrocarbon oil at −150 °C (123 K). Crystal data were obtained using an Enraf-Nonius Kappa CCD. X-ray data were processed using the DENZO program [54]. Structural solution and refinement was carried out using the SHELX suite of programs [55,56] with the graphical interface X-SEED [57]. All hydrogen atoms were placed in calculated positions using the riding model. Crystal data and refinement parameters for all lithium and sodium complexes are compiled in Tables 1 and 3 respectively.

For compound **2**, two THF carbons of both molecular units disordered (C48 and C50). Disorder modelled as 64:36%, 50:50%, 61:39% and 78:22% occupancy, respectively (units A and B). Also, methyl of ethyl group attached to aromatic of μ$_2$:η^1:η^1-*N*,*C*,*N*′-FPhEt (C20C/D and C18E/F) disordered in both molecular units. Modelled as 52:48% and 64:36% occupancy, respectively. Carbons 48D and 50F required ISOR (0.01) refinement to obtain satisfactory thermal parameters.

For compound **8**, one ethyl group (C8A/D) disordered over two sites. These were modelled as 52:48% occupancy. One THF molecule also exhibited disorder across a single methylene (C24C/D). This was modelled successfully with 66:34% occupancy.

For compound **9**, carbons 32 and 36 were found to be slightly prolate. Attempted modelling of disorder failed to provide satisfactory thermal parameters. Inversion of asymmetric unit attempted due to flack parameter of 0.1815 (esd 0.4224). This gave a value approaching 1.0, and hence the original model was retained.

For compound **12**, one methyl of an isopropyl (C12) disordered over two sites of partial occupancy. Modelled successfully with 68:32% occupancy. Also, one methylene of a DME disordered (C16). Modelled successfully with 75:25% occupancy.

6. Supplementary material

Crystallographic data (excluding structure factors) for the structures reported in this paper have been deposited with the Cambridge Crystallographic Data Centre as supplementary numbers 228551–228560. Copies of the data can be obtained free of charge on application to CCDC, 12 Union Road, Cambridge, CB2 1EZ, UK (fax: +44-1223-336033; e-mail: deposit@ccdc.cam.ac.uk).

7. Conclusion

We have successfully demonstrated that the placement of alkyl groups on the 2- and 6-aryl positions of lithium and sodium *N*,*N*′-di(aryl)formamidinates induces disruption of assembly yielding some unprecedented coordination and binding motifs. In particular instances, especially where the coordination mode is asymmetric, the binding is retained in solution (^{1}H NMR). For THF solvated FPhEt complexes (**2** and **8**) this renders the first amidinate/guanidinate complexes to display Li or Na arene-C contacts. These ensue as one or more of the ligands concerned assumes an *E*-*syn*/*Z*-*anti* [23] isomeric form. In doing so, these structural findings are somewhat consistent with observations for related potassium *N*,*N*′-di(aryl)formamidinate chemistry [16,17]. In the case of HFIso, metallation by lithium or sodium, irrespective of the donor coordination environment, renders monomeric species. For HFXyl, metallation using butyl lithium permits the formation of dimeric 'lantern' type species (using the FMes and FPhEt examples to extrapolate for compound **4**), the effect of the increasing steric bulk at the 2- and 6-aryl position merely inducing greater structural contortion of the eight-membered metallocycles that appear prominently in anionic β-dinitrogen ligand lithium chemistry [32]. For sodium metallation, failure to isolate crystalline samples of **7** (empirical composition by ^{1}H NMR [Na(FXyl)(THF)$_2$]) leave its structural composition open to conjecture, however, the DME analogue (**10**) exists as a monomer in the solid state whilst the lack of asymmetry in ^{1}H NMR spectra of **7**, as per **8**, debases the possibility of aryl-C contacts. The lithiation of HFPhEt in DME renders a μ$_2$:η^1:η^1-bound dimer similar to less bulky *N*,*N*′-di(aryl)formamidinates [8,11]. A similar composition (μ$_2$:η^2:η^1- instead of μ$_2$:η^1:η^1-) is observed for the sodium analogue, upon recrystallisation from hexane, which permits loss of one equivalent of DME. These results serve to establish that lithium and sodium metallation of these ligands using standard

laboratory reagents occurs without innate suppression, unlike the potassium metallation of related species [16,17].

We are currently investigating the lanthanoid *N*,*N*′-di(aryl)formamidinate chemistry of HFXyl, HFMes, HFPhEt and HFIso as well as related potassium chemistry. The results of these studies will form the basis of forthcoming publications.

Acknowledgements

The authors thank the Australian Research Council (ARC) for continued financial support and the EPRSC (UK) for a studentship for AJD.

References

[1] J.R. Su, X.W. Li, R.C. Crittendon, G.H. Robinson, J. Am. Chem. Soc. 119 (1997) 5471.
[2] B. Twamley, P.P. Power, Angew. Chem., Int. Ed. Engl. 39 (2000) 3500.
[3] G.H. Robinson, Adv. Organomet. Chem. 47 (2001) 283.
[4] P.P. Power, Chem. Commun. (2003) 2091.
[5] N.J. Hardman, R.J. Wright, A.D. Phillips, P.P. Power, J. Am. Chem. Soc. 125 (2003) 2667.
[6] L.H. Pu, A.D. Phillips, A.F. Richards, M. Stender, R.S. Simons, M.M. Olmstead, P.P. Power, J. Am. Chem. Soc. 125 (2003) 11626.
[7] See for example: R.T. Boeré, V. Klassen, G. Wolmershauser, J. Chem. Soc., Dalton Trans. (1998) 4147.
[8] M.L. Cole, P.C. Junk, L.M. Louis, J. Chem. Soc., Dalton Trans. (2002) 3906.
[9] M.L. Cole, D.J. Evans, P.C. Junk, M.K. Smith, Chem. Eur. J. 9 (2003) 415.
[10] J. Baldamus, C. Berghof, M.L. Cole, D.J. Evans, E.-M. Hey-Hawkins, P.C. Junk, J. Chem. Soc., Dalton Trans. (2002) 4185.
[11] J. Baldamus, C. Berghof, M.L. Cole, E.-M. Hey-Hawkins, P.C. Junk, L.M. Louis, Eur. J. Inorg. Chem. (2002) 2878.
[12] Alternatives to ubiquitous cyclopentadienyl systems have been pursued fervently in lanthanide chemistry. Amides have become the most successful of these alternatives owing to their ease of derivatisation and commensurate charge characteristics when associated with electropositive metals. For a review of this area see: R. Kempe, Angew. Chem., Int. Ed. Engl. 39 (2000) 468.
[13] J. Barker, M. Kilner, Coord. Chem. Rev. 133 (1994) 219.
[14] F.T. Edelmann, Coord. Chem. Rev. 137 (1994) 403.
[15] P.J. Bailey, S. Pace, Coord. Chem. Rev. 214 (2001) 91.
[16] J. Baldamus, C. Berghof, M.L. Cole, D.J. Evans, E.-M. Hey-Hawkins, P.C. Junk, J. Chem. Soc., Dalton Trans. (2002) 2802.
[17] M.L. Cole, P.C. Junk, J. Organomet. Chem. 665 (2003) 33.
[18] P.B. Hitchcock, M.F. Lappert, D.-S. Liu, J. Organomet. Chem. 488 (1995) 241.
[19] P.B. Hitchcock, M.F. Lappert, M. Layh, J. Chem. Soc., Dalton Trans. (1998) 3113.
[20] G.R. Giesbrecht, A. Shafir, J. Arnold, J. Chem. Soc., Dalton Trans. (1999) 3601.
[21] R.T. Boeré, M.L. Cole, P.C. Junk, E.G. Robertson, M.K. Smith, unpublished material.
[22] In isolation, FTIR data for lithium complexes 1-6 suggest there may be a correlation between the binding mode adopted, beit bridging or chelating, and the wavenumber of the C=N stretch. However, upon analysis of analogous absorptions for complexes 7-12 (vide infra), and consideration of the mixed tautomerisation of compounds 2 and 8, no definitive relationship between this stretch and the binding mode, or the placement of the aromatic groups to the NCN backbone, could be established.
[23] S. Patai, Z. Rappoport (Eds.), Using the Nomenclature of C.L. Perrin in The Chemistry of the Amidines and Imidates, vol. 2, Wiley, Chichester, UK, 1991, p. 152 (Chapter 3).
[24] Solvent dependency was originally put forward as a key reason for the notable absence of structurally authenticated alkali metal amidinate species, see: F.A. Cotton, S.C. Haefner, J.H. Matonic, X.P. Wang, C.A. Murillo, Polyhedron 16 (1997) 541.
[25] The Cambridge Crystallographic Structural Database (CCSD version 1.5, November 2002) contains 39 examples where tetrahydrofuran bridges two or more metal centres.
[26] From a survey of the Cambridge Crystallographic Structural Database (CCSD version 1.5, November 2002).
[27] For example see references [27–31]: M. Niemeyer, P.P. Power, Inorg. Chem. 35 (1996) 7264.
[28] B. Eichhorn, H. Nöth, T. Seifert, Eur. J. Inorg. Chem. (1999) 2355.
[29] B.E. Eichler, P.P. Power, Inorg. Chem. 39 (2000) 5444.
[30] G.W. Rabe, R.D. Sommer, A.L. Rheingold, Organometallics 19 (2000) 5537.
[31] P.C. Andrews, G.B. Deacon, C.M. Forsyth, N.M. Scott, Angew. Chem. Int. Ed. Engl. 40 (2001) 2109.
[32] From a survey of the Cambridge Crystallographic Structural Database (CCSD version 1.5, November 2002) there are 42 identified examples of this structure type. For "chair" example see; A.D. Bond, F. Garcia, K. Jantos, G.T. Lawson, M. McPartlin, D.S. Wright, Chem. Commun. (2002) 1276;
For "boat" example see;W.M. Boesveld, P.B. Hitchcock, M.F. Lappert, Chem. Commun. (1997) 2091.
[33] See for example: C. Knapp, E. Lork, P.G. Watson, R. Mews, Inorg. Chem. 41 (2002) 2014;
J. Barker, D. Barr, N.D.R. Barnett, W. Clegg, I. Cragg-Hine, M.G. Davidson, R.P. Davies, S.M. Hodgson, J.A.K. Howard, M. Kilner, C.W. Lehmann, I. Lopez-Solera, R.E. Mulvey, P.R. Raithby, R. Snaith, J. Chem. Soc., Dalton Trans. (1997) 951.
[34] T. Chivers, M. Parvez, G. Schatte, J. Organomet. Chem. 550 (1998) 213.
[35] P.J. Bailey, A.J. Blake, M. Kryszczuk, S. Parsons, D. Reed, Chem. Commun. (1995) 1647.
[36] J.A.R. Schmidt, J. Arnold, J. Chem. Soc., Dalton Trans. (2002) 2890.
[37] I. Cragg-Hine, M.G. Davidson, F.S. Mair, P.R. Raithby, R. Snaith, J. Chem. Soc., Dalton Trans. (1993) 2423.
[38] J.A.R. Schmidt, J. Arnold, Chem. Commun. (1999) 2149.
[39] M.F. Lappert, P.P. Power, A.R. Sanger, R.C. Srivastava, Metal and Metalloid Amides, Ellis Horwood Ltd., Chichester, England, 1980.
[40] A.M. Sapsa, P.V.R. Schleyer (Eds.), Lithium Chemistry: A Theoretical and Experimental Overview, Wiley-Interscience, New York, USA, 1995.
[41] G.D. Whitener, J.R. Hagadorn, J. Arnold, J. Chem. Soc., Dalton Trans (1999) 1249.
[42] D. Stalke, M. Wedler, F.T. Edelmann, J. Organomet. Chem. 431 (1992) C1.
[43] W.M. Boesveld, P.B. Hitchcock, M.F. Lappert, H. Nöth, Angew. Chem., Int. Ed. Engl. 39 (2000) 222.
[44] Radii given those of six-coordinate alkali metals: E. Fluck, K.G. Heumann, Periodic Table of the Elements, VCH, Weinheim, Germany, 1991.
[45] See for example refence [1] and: J.M. Smith, R.J. Lachicotte, K.A. Pittard, T.R. Cundari, G. Lukat-Rodgers, K.R. Rodgers, P.L. Holland, J. Am. Chem. Soc. 123 (2001) 9222.
[46] See for example: C.H. Haar, C.L. Stern, T.J. Marks, Organometallics 15 (1996) 1765.

[47] D.G. Dick, R. Duchateau, J.J.H. Edema, S. Gambarotta, Inorg. Chem. 32 (1993) 1959.
[48] Z. Lu, G.P.A. Yap, D.S. Richeson, Organometallics 20 (2001) 706.
[49] A. Recknagel, F. Knosel, H. Gornitzka, M. Noltemeyer, F.T. Edelmann, J. Organomet. Chem. 417 (1991) 363.
[50] J.R. Hagadorn, J. Arnold, Organometallics 15 (1996) 984.
[51] M. Karl, A. Dashti-Mommertz, B. Neumüller, K. Dehnicke, Z. Anorg. Allg. Chem. 624 (1998) 355.
[52] S. Chadwick, U. Englich, K. Ruhlandt-Senge, Organometallics 16 (1997) 5792.
[53] R.M. Roberts, J. Org. Chem. 14 (1949) 277.
[54] Z. Otwinowski, W. Minor, in: C.W. Cater, R.M. Sweet (Eds.), Processing of X-ray Diffraction Data Collected in Oscillation Mode, Methods in Enzymology, 276: Macromolecular Crystallography, Part A, vol. 307, 1997, Academic Press.
[55] G.M. Sheldrick, SHELXL-97, University of Göttingen, Germany, 1997.
[56] G.M. Sheldrick, SHELXS-97, University of Göttingen, Germany, 1997.
[57] L.J. Barbour, J. Supramol. Chem. 1 (2001) 189.